Journal of
Applied Physics

Interfacial properties of penta-graphene-metal contacts

Cite as: J. Appl. Phys. **125**, 065308 (2019); https://doi.org/10.1063/1.5085414
Submitted: 12 December 2018 . Accepted: 29 January 2019 . Published Online: 14 February 2019

Arzoo Hassan, Yaguang Guo, Qian Wang, Yoshiyuki Kawazoe, and Puru Jena

AIP Publishing

Journal of
Applied Physics

ARTICLE

scitation.org/journal/jap

Interfacial properties of penta-graphene-metal contacts

Cite as: J. Appl. Phys. **125**, 065308 (2019); doi: 10.1063/1.5085414
Submitted: 12 December 2018 · Accepted: 29 January 2019 ·
Published Online: 14 February 2019

View Online Export Citation CrossMark

Arzoo Hassan,[1] Yaguang Guo,[1] Qian Wang,[1,a)] Yoshiyuki Kawazoe,[2] and Puru Jena[3]

AFFILIATIONS

[1] Center for Applied Physics and Technology, Department of Materials Science and Engineering, BKL-MEMD, College of Engineering, Peking University, Beijing 100871, China
[2] New Industry Creation Hatchery Center, Tohoku University, Sendai 980-8577, Japan
[3] Department of Physics, Virginia Commonwealth University, Richmond, Virginia 23284, USA

[a)] **E-mail:** qianwang2@pku.edu.cn

ABSTRACT

Novel properties of penta-graphene (PG) have stimulated great interest in exploring its potential for device applications. Here, we systematically study the interfacial properties of the heterojunctions constructed by stacking PG on several metal substrates (Ag, Al, Au, Cr, Cu, Pd, and Ti), which are commonly used in field-effect transistors. We consider PG as the channel material because of its semiconducting feature, while treating the metal surfaces as the electrodes. Based on first principles calculations, we show that PG preserves its pentagonal feature with some small distortions when deposited on the metal substrates but undergoes metallization due to the chemical bonding between PG and the metal surfaces. We evaluate the device potential of these PG-metal contacts by studying their tunneling barriers, orbital overlaps, and Schottky barriers. We find that PG forms an n-type Schottky barrier when in contact with Al, Cu, and Ti, but forms a p-type Schottky barrier when supported on Ag, Au, Cr, and Pd. Our study sheds light on the design and fabrication of PG-based electronic devices.

I. INTRODUCTION

Penta-graphene (PG) is particularly interesting due to its exotic atomic configuration and remarkable properties.[1] Unlike graphene, where hexagonal carbon rings serve as the structural motif, PG is composed exclusively of carbon pentagons, displaying an array of intriguing properties that even outperformed graphene.[1–4] For instance, it possesses some novel mechanical properties,[1,4] such as a negative Poisson's ratio and an ultrahigh ideal strength. It also exhibits unique thermal conductivity and metal-free catalytic activity.[5–8] More importantly, PG has a fundamental energy bandgap of 3.25 eV,[1,9–11] which is close to that of ZnO and GaN, showing the feature of a wide-gap semiconductor. Thus, PG can be expected to have potential applications in nano electronic devices.

In a real device, such as a field-effect transistor (FET), a contact between the channel material and metal is usually required to inject an appropriate type of carrier into the conduction or valance bands of the semiconducting channel material. However, the biggest challenge that masks the intrinsic properties of the semiconductor is the lack of a low resistance metal contact. For example, experiments show that a large Schottky barrier appears in the contacts between MoS_2 and Au, Pt, Sc, and Pd,[12,13] which cannot be easily modulated because of the Fermi level pinning induced by the metallization of MoS_2.[14,15] To overcome such issues in the PG-based device, we explored an all-carbon heterojunction composed of PG and graphene,[16] where graphene is considered as the metal electrode. We found that the intrinsic electronic properties of both PG and graphene are well preserved after they are stacked together, forming a van der Waals (vdW) heterojunction. An n-type Schottky barrier is formed at the contact interface, which can be effectively reduced by electrostatic gating or doping graphene with nitrogen atoms. However, in terms of the process of its robustness and electrical reliability, bulk metals are still the first choice for practical device applications, as compared to using two-dimensional (2D) monolayers. It is, therefore, highly desirable to explore suitable metals and the contact configurations that can have maximum potential to form low-resistance PG-metal contacts. At present, no such research has been reported. This motivates us to carry out this study.

In this work, using the density functional theory (DFT), we have systematically studied the geometric and electronic properties of the heterojunctions constructed by vertically stacking the PG monolayer and metal (Ag, Al, Au, Cu, Cr, Pd, and Ti) surfaces, respectively. The issue of lattice mismatch between PG and the metal surfaces is taken care of by using our in-house code.[17] To study device performance, the interface properties including electrostatic potential, electronic structures, and band alignment have also been investigated. We have demonstrated that apart from choosing a metal with proper work function, the interface between PG and the metal surface plays an important role in achieving a low resistant contact.

II. COMPUTATIONAL METHODS

A. Interface modeling

According to the Schottky-Mott rule,[18] a metal with very large or very small work function is needed to form a low-barrier contact. We selected seven metals, including Ag, Al, Au, Cu, Cr, Pd, and Ti, because they are commonly used in transistor junctions, and their work functions cover a wide range.[19] To construct PG-metal heterojunctions, we chose Ag, Au, and Cr (110) surfaces, Pd and Cu (111) surfaces, and Ti (0001) surface, respectively, to match the PG monolayer, as these are the most probable orientations found in experiments. We have used a five-layer slab model with the bottom three layers of the metal atoms fixed at their bulk position to simulate the metal surfaces. To study the effect of film thickness and minimize the computational cost, we limited tests to three to seven-layer slabs. We then vertically stacked PG and the metal surfaces together to build the heterojunctions, respectively. Since the symmetry and lattice constants of PG and those of the selected metal surfaces are different from each other, we have used our in-house code[17] to generate the heterostructure supercells by setting the lattice mismatch less than 2% and the total number of atoms to less than 300. A detailed procedure for generating the supercells is given in Fig. S1 in the supplementary material. A vacuum space of 20 Å in the normal direction of the interfaces is added to avoid spurious interaction between the periodic images.

B. DFT calculations

Our first principles calculations within the framework of DFT were carried out using the Vienna *ab initio* Simulation Package (VASP), employing the projector augmented wave (PAW) pseudopotentials[20,21] and the Perdew-Burke-Ernzerhof (PBE) exchange-correlation functional.[22] To correctly describe the effect of vdW interactions, we used a dispersion-corrected DFT method (optB88-vdW). The plane-wave cutoff energy is set to 500 eV for all calculations. The Brillouin zone is sampled with $5 \times 5 \times 1$ Monkhorst-Pack special *k*-point meshes[23] for Ag, Al, and Au, $9 \times 1 \times 1$ for Cu and Ti, $1 \times 1 \times 1$ for Pd, and $7 \times 7 \times 1$ for Cr, respectively. All studied heterojunctions are relaxed until the force and energy on each atom is less than 0.01 eV/Å and 1×10^{-4} eV, respectively.

III. RESULTS

Three major factors determine the electronic transparency of the contact in a metal semiconductor junction, which include (1) interface geometry, (2) tunneling barrier, and (3) Schottky barrier. A favorable interface structure requires a small lattice mismatch, which can maximize the orbital overlap between both sides. The tunneling barrier should be as narrow and as low as possible to increase the tunneling probability, thus maximizing the current injection. The height of the Schottky barrier should also be low so that the charge transfer can be more efficient. In the following, we evaluate the interfacial properties of the PG-metal junctions by analyzing each of these factors one by one.

In Fig. 1, we show the geometric structures of the optimized contacts. Because of the small lattice mismatch (< 2%), after geometry optimization, the original structure of PG is well preserved on all of the selected metal substrates, implying that the lattice strain is negligible in these heterostructures. To study the interaction between PG and the metal surface, interlayer distance (*d*) is measured for each of the optimized contacts (see Table I), which is defined as the average distance between the top layer of metal and the bottom layer of PG. We find that PG strongly bonds with the Au, Al, Pd, Cr, and Cu surfaces, respectively, as reflected by the fact that the calculated average interlayer distance of these contacts is approximately equal to or shorter than the sum of C and metal atom covalent radii. For example, *d* for PG-Au contact is 1.57 Å, which is 0.54 Å shorter than the sum of C and Au covalent radii. However, we note that the interaction between MoS_2 and Au is relatively weak as *d* is longer than the sum of S and Au covalent radii in the MoS_2-Au contact.[24] This is because unlike fully saturated sulfur in MoS_2, the sp^2 hybridized C atoms in PG are not fully saturated, which results in a stronger chemical bonding. Because of the short distance between PG and the metal surfaces, a large orbital overlap exists in these contacts.

To characterize the bond strength in these contacts, we calculate the binding energy E_b for each of them. This is defined as

$$E_b = (E_{PG} + E_M - E_{PG-M})/N, \tag{1}$$

where E_{PG}, E_M, and E_{PG-M}, respectively, represent the total energies of PG, metal surface, and PG-metal heterojunction, respectively, and N represents the number of atoms of PG in the heterojunction supercell. The calculated binding energies for PG-M (M = Ag, Al, Au, Cr, Cu, Pd, and Ti) heterojunctions are 0.85, 0.45, 0.77, 1.63, 0.73, 0.27, and 0.66 eV, respectively. The PG-M (M = Au, Cr, and Cu) contacts have larger binding energies of 0.77, 1.63, and 0.73 eV, respectively, that are larger

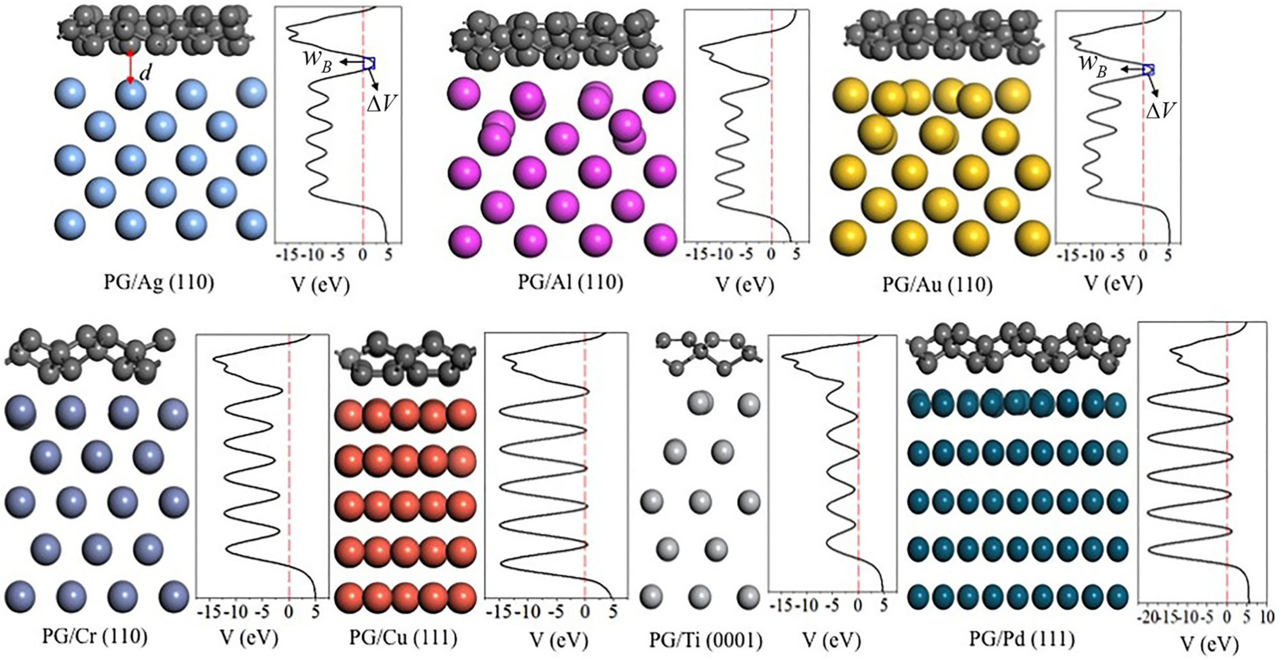

FIG. 1. Side views of the optimized PG-M (M = Ag, Al, Au, Cr, Cu, Pd, and Ti) contacts and the average electrostatic potentials in the normal direction to the interfaces. ΔV and w_B are the tunneling barrier height and width, respectively, and d is the interlayer distance between the bottom layer of PG and top layer of the metal. The Fermi level is shifted to zero.

than those of PG-M (M = Al, Ti, and Pd) contacts whose binding energies lie in the range of 0.27 and 0.66 eV. On the other hand, the interlayer distance of the former group ($1.57 \leq d \leq 2.11$ Å) is larger than those of the latter group ($2.13 \leq d \leq 2.37$ Å). In contrast, graphene-M (M = Al, Cu, Ag, Au, and Pt) contacts lead to a much weaker binding ($E_b \leq 0.04$ eV) and a larger equilibrium separation ($d \approx 3.3$ Å).[25] Our results imply that the interaction between PG and the metal surfaces is stronger than that of graphene and metal surfaces, suggesting that PG is more reactive toward the metals than the graphene.[26,27]

TABLE I. Calculated interfacial properties of the PG-M (Ag, Al, Au, Cu, Cr, Pd, and Ti) contacts, including the average interlayer distance (d in Å) between the PG monolayer and metal surface, binding energy per carbon atom of PG (E_b in eV), tunneling barrier height (ΔV in eV), tunneling barrier width (w_B in Å), tunneling probability (T_B in %), and the Schottky barrier height for electrons (Φ_e in eV) and holes (Φ_h in eV) in the lateral direction. Work functions of the pure metals (WF in eV), and heterojunctions (WF_H in eV) are also given.

	Ag	Al	Au	Cr	Cu	Pd	Ti
d	2.52	2.13	1.57	2.07	2.11	2.10	2.37
E_b	0.85	0.45	0.77	1.63	0.73	0.27	0.66
WF	4.38	4.14	5.16	5.06	5.00	5.41	4.79
WF_H	5.37	4.39	5.20	5.09	4.99	5.37	4.86
ΔV	2.20	0	1.97	0	0.74	0.55	0
w_B	0.80	0	0.60	0	0.30	0.30	0
T_B	29.73	100	42.28	100	76.81	76.66	100
Φ_e	1.12	1.20	2.01	1.90	1.47	2.18	1.60
Φ_h	1.09	2.07	1.26	1.37	1.80	1.09	1.67

Next, we calculate the energy barriers at the PG-metal interfaces to evaluate their device performance. A schematic image of the PG-based two-probe FET model is plotted in Fig. 2. A tunneling barrier (TB) and a vertical Schottky barrier (Φ_v) may exist at the interface (B) between the metal surface and PG monolayer, depending on the strength of their binding interaction. A lateral Schottky barrier (Φ_L) can appear at interface D between the heterojunction and the PG channel region. We first calculate the electrostatic potential to analyze the tunneling barrier. From the potential profile, as shown in Fig. 1, the PG-M (M = Al, Cr, and Ti) contacts have no tunneling barriers, as their potential energies do not cross over the Fermi level. However, there is an obvious tunneling barrier in PG-M (M = Ag, Au, Cu, and Pd) with a barrier height of 2.20, 1.97, 0.74, and 0.55 eV, respectively. The tunneling barrier can be characterized by its height (ΔV) and width (w_B). Since the real potential barrier has an irregular shape, we assume a square potential barrier to estimate the tunneling probability (T_B) by using the WKB equation[27,28]

$$T_B = \exp\left(-2\frac{\sqrt{2m\Delta V}}{\hbar} \times w_B\right), \tag{2}$$

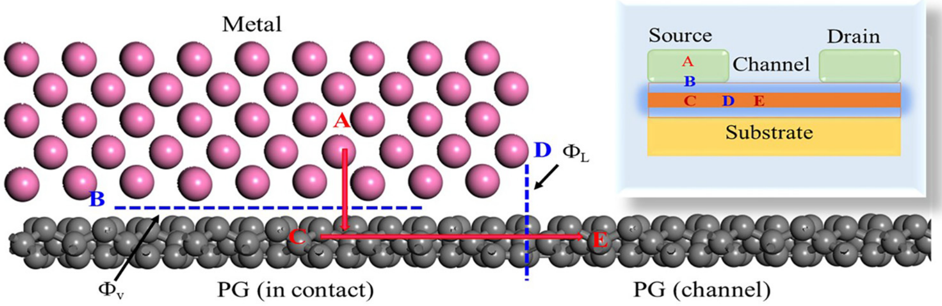

FIG. 2. Schematic diagram of the PG-metal heterojunction. A, C, and E denote the metal, PG contact, and the channel region, respectively, while B and D are the two interfaces separating them. The red arrows show the pathway of charge carrier injection from the metal electrode to the PG channel (A → B → C → D → E). Φ_v and Φ_L denote the vertical and lateral Schottky barriers, respectively. The right figure is a schematic diagram of a heterojunction-based FET, showing the source, drain, and channel regions.

where m is the mass of the free electron and ħ is the reduced Planck's constant. Obviously, the tunneling possibility is 100% for the PG-M (M = Al, Cr, and Ti) contacts, while that for the PG-M contacts with M = Ag, Au, Cu, and Pd it is 29.73, 42.28, 76.81, and 76.66%, respectively. The small physical separation d between the PG layer and Au, Cr, Cu, or Pd metal surface leads to a small tunneling barrier height ΔV and strong orbital overlap. This is the case with the metal contacts of monolayer transition metal dichalcogenide (TMD) semiconductors.[29] Tunneling probability of a weak-bonding system is usually smaller than that of a strong bonding one. Our calculated results show that the PG-Al, PG-Cr, and PG-Ti contacts can be expected to have excellent electron injection efficiency because of the strong metallization and absence of tunneling barrier at the their interfaces.

Besides the tunneling barrier, another important key factor that determines the contact resistance of a heterojunction is the Schottky barrier.[30] To study this, we calculate the band structure of the free-standing PG monolayer and the projected band structures of PG in these contacts. The results are plotted in Fig. S2 in the supplementary material. It clearly shows that the band structures of PG supported on all

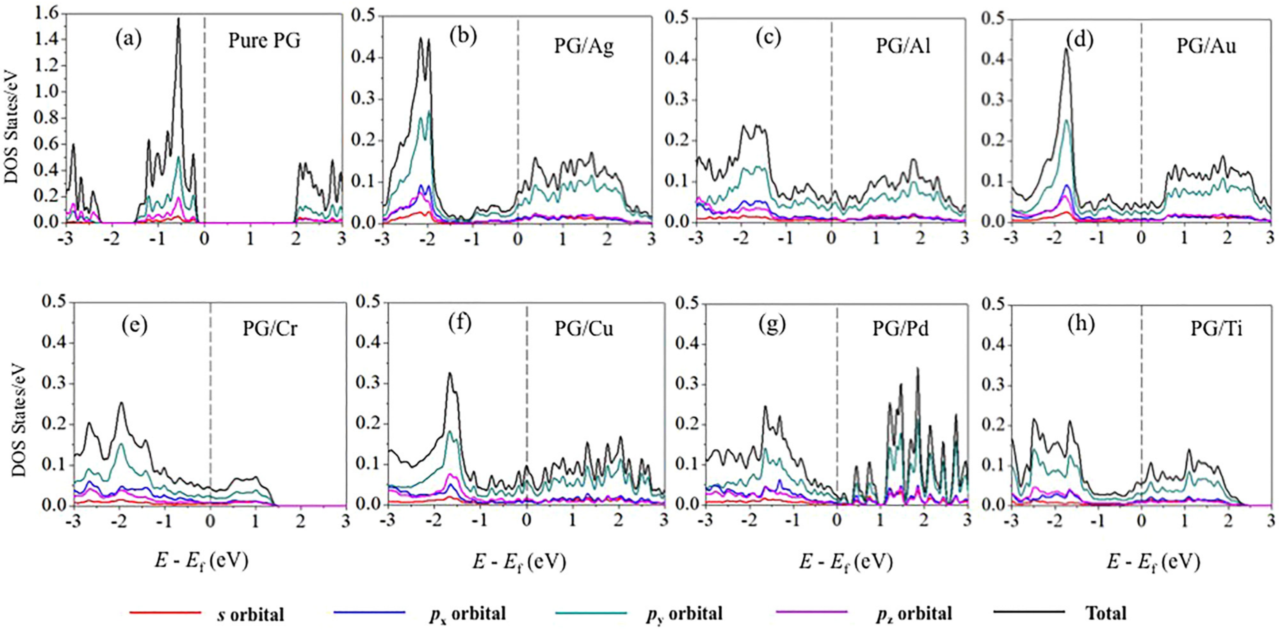

FIG. 3. (a) DOS of the pristine PG monolayer and (b)–(h) are the DOS contributed from PG in PG-M (M = Ag, Al, Au, Cu, Cr, Pd, and Ti) heterojunctions. The Fermi energy is set to zero.

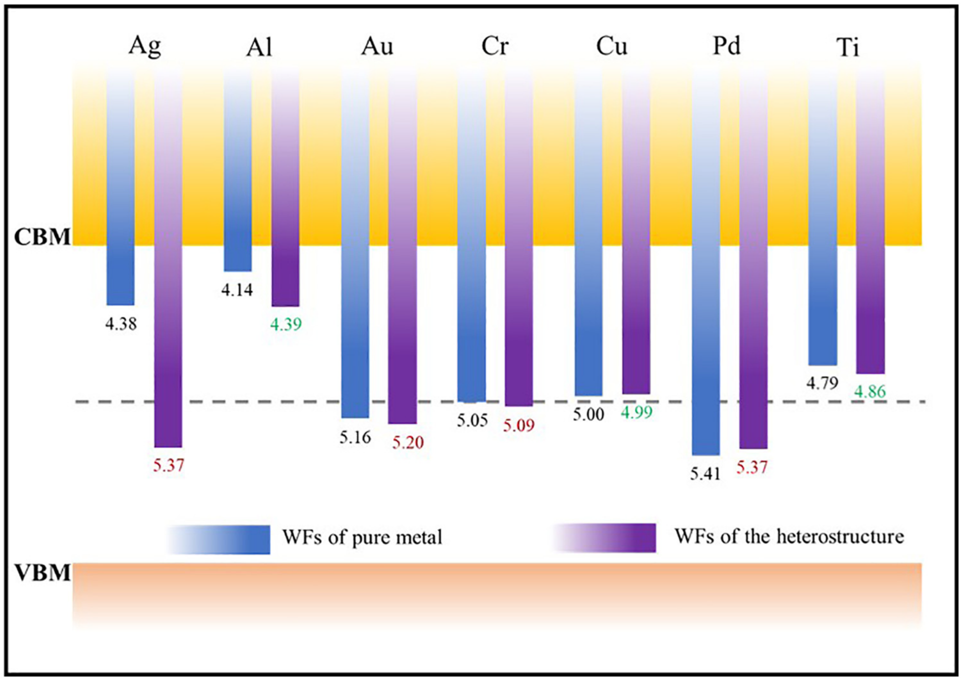

FIG. 4. Band alignment of the contacts by using the work function (WF in eV) of the pure metals shown in blue bars, and the work function of the heterojunctions shown in purple bars. CBM and VBM denote the energies of the conduction band minimum and the valence band maximum of PG, respectively.

of the metal substrates are significantly perturbed because of the chemical bonding between the carbon and metal atoms. However, for graphene-metal contacts, the projected band structures of graphene on Al, Ag, Au, and Cu substrates are much less perturbed, where the band dispersions as well as the Dirac points can be clearly identified.[25] This is very different from the PG-metal contacts studied here. This, once again, suggests that the interactions between PG and the metal surfaces are stronger than that between graphene and metal surfaces.[25,26,31] The band hybridization in PG-M (M = Al, Au, Cr, and Pd) is more intense as compared to that in PG-M (M = Ag, Cu, and Ti). The energy bandgap of pristine PG in all the contact disappears, where the new bands are induced by the orbital overlaps, and extend into the original gap of PG. This implies that PG undergoes metallization, thus the vertical Schottky barrier (Φ_v) at the interface (B) between PG and the metal surface vanishes. From Fig. S2 in the supplementary material, we further infer that the electrons in the overlap states of the band structures of the PG-Ag, PG-Cu, and PG-Ti contacts are delocalized, because most of their energy bands

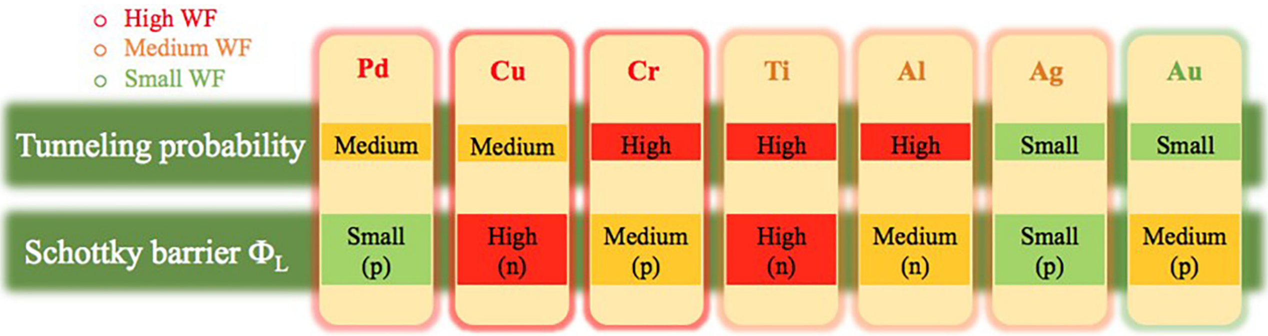

	Pd	Cu	Cr	Ti	Al	Ag	Au
Tunneling probability	Medium	Medium	High	High	High	Small	Small
Schottky barrier Φ_L	Small (p)	High (n)	Medium (p)	High (n)	Medium (n)	Small (p)	Medium (p)

FIG. 5. Summary of the electron injection efficiency of PG-metal contacts in terms of tunneling probability and Schottky barrier.

have high curvatures, indicating a small charge effective mass. Therefore, the conductivity of PG in these contacts is not degraded by the metal atoms for an efficient carrier transport, which is good for carrier injection from metal to PG.

In order to further confirm the metallization of PG in the heterojunctions, we also plot the density of states (DOS) for the PG-metal contacts in Fig. 3. One can see that a large number of metal-induced-gap-states appear in the original bandgap of pristine PG, especially at the Fermi level, and the bandgaps disappear in all of the seven systems, resulting from the hybridization of the energy bands. For all of the contacts, the s, p_x, and p_z states are nearly uniformly distributed with small contributions to the states near the Fermi level. The py orbitals make the major contribution to the original bandgap of PG. The band hybridizations in these PG-metal contacts are different from those of graphene-metal systems where the hybridized bands are solely comprised of p_z.[25]

We then calculate the lateral Schottkky barrier (Φ_L) following the same precedure as in our provious study.[16] The Schottky barrier height (SBH) is defined as

$$\Phi_e = E_{CBM} - E_F, \Phi_h = E_F - E_{VBM}, \tag{3}$$

where Φ_e and Φ_h are the lateral SBHs for electrons and holes, E_F represents the Fermi level of the heterojunction, while E_{CBM} and E_{VBM} denote the energies of the conduction band minimum (CBM) and the valence band maximum (VBM) of the PG semiconductor, respectively. The calculated results are plotted in Fig. 4. Note that except for Ag and Al, the work functions (WFs) of the metals change slightly after the contacts are made with PG, respectively. According to the band alignment, PG forms p-type Schottky barriers when contacted with Ag, Au, Cr, and Pd substrates because the position of the Fermi level of the interfacial system is close to the VBM of PG. The corresponding Schottky barrier heights are 1.09, 1.26, 1.37, and 1.09 eV, respectively. On the other hand, it forms the n-type Schottky barrier when in contact with Al, Cu, and Ti, because the Fermi level is close to the CBM of PG. Thus the conduction is through electrons in these transistor models.

IV. DISCUSSION

Based on the above analysis of tunneling and Schottky barriers, we summarize the main results in Fig. 5. One can see that the PG-M (M = Al, Cr, and Ti) contacts would have excellent electron injection properties because of the strong metallization and the absence of a tunneling barrier at the interfaces. This can enhance the performance when used as a FET device. PG-Al is a more favorable contact due to the formation of the n-type contact with a SBH of 1.20 eV. Although PG-Cr and PG-Ti contacts undergo strong metallization and have 100% tunneling possibility, the presence of SBH of 1.37 and 1.60 eV in the lateral direction, respectively, is relatively higher for both n-type and p-type contacts. While the PG-Au contact is a superior contact relative to that of the PG-Ti contact in terms of a lower SBH of 1.26 eV, the presence of an unexpected tunneling barrier in PG-Au would degrade its performance. Similarly, although the PG-Cu heterojunction also forms an n-type contact, the presence of a tunneling barrier at the interface and a SBH of 1.47 eV would also degrade its performance. Both PG-Ag and PG-Pd heterojunctions form a p-type contact with a SBH of 1.09 eV. However, the PG-Pd contact is superior to the former because of its higher tunneling possibility. Therefore, we conclude that Al and Pd are the best n-type top-contact and the best p-type contact metal for PG, respectively. All the calculated parameters regarding the geometrical stability and contact evaluations are also summarized in Table I.

SUPPLEMENTARY MATERIAL

See the supplementary material for the procedure for generating heterojunction supercells and electronic band structures of PG-metal contacts.

ACKNOWLEDGMENTS

This work was partially supported by grants from the National Key Research and Development Program of China (Grant Nos. 2016YFE0127300 and 2017YFA0205003), the National Science Foundation China (Grant No. NSFC-21773004), and supported by the High-Performance Computing Platform of Peking University China. P.J. acknowledges support by the U.S. DOE, Office of Basic Energy Sciences, Division of Material Sciences and Engineering under Award No. DE-FG02-96ER45579.

REFERENCES

[1] S. Zhang, J. Zhou, Q. Wang, X. Chen, Y. Kawazoe, and P. Jena, Proc. Natl. Acad. Sci. U.S.A. **112**, 2372 (2015).
[2] T. Stauber, J. Beltrán, and J. Schliemann, Sci. Rep. **6**, 22672 (2016).
[3] H. Einollahzadeh, R. Dariani, and S. Fazeli, Solid State Commun. **229**, 1 (2016).
[4] H. Sun, S. Mukherjee, and C. V. Singh, Phys. Chem. Chem. Phys. **18**, 26736 (2016).
[5] F. Q. Wang, J. Yu, Q. Wang, Y. Kawazoe, and P. Jena, Carbon **105**, 424 (2016).
[6] F. Q. Wang, J. Liu, X. Li, Q. Wang, and Y. Kawazoe, Appl. Phys. Lett. **111**, 192102 (2017).
[7] X. Wu, V. Varshney, J. Lee, T. Zhang, J. L. Wohlwend, A. K. Roy, and T. Luo, Nano Lett. **16**, 3925 (2016).
[8] H. Liu, G. Qin, Y. Lin, and M. Hu, Nano Lett. **16**, 3831 (2016).
[9] R. Krishnan, W.-S. Su, and H.-T. Chen, Carbon **114**, 465 (2017).
[10] M.-Q. Le, Comp. Mater. Sci. **136**, 181 (2017).
[11] G. Berdiyorov, G. Dixit, and M. Madjet, J. Phys. Condens. Matter **28**, 475001 (2016).
[12] B. Radisavljevic, A. Radenovic, J. Brivio, I. V. Giacometti, and A. Kis, Nat. Nanotechnol. **6**, 147 (2011).
[13] M. Fontana, T. Deppe, A. K. Boyd, M. Rinzan, A. Y. Liu, M. Paranjape, and P. Barbara, Sci. Rep. **3**, 1634 (2013).
[14] C. Gong, L. Colombo, R. M. Wallace, and K. Cho, Nano Lett. **14**, 1714 (2014).
[15] S. Das, H.-Y. Chen, A. V. Penumatcha, and J. Appenzeller, Nano Lett. **13**, 100 (2012).
[16] Y. Guo, F. Q. Wang, and Q. Wang, Appl. Phys. Lett. **111**, 073503 (2017).
[17] Y. Guo, W. A. Saidi, and Q. Wang, 2D Mater. **4**, 035009 (2017).
[18] P. Blom, R. Wolf, J. Cillessen, and M. Krijn, Phys. Rev. Lett. **73**, 2107 (1994).
[19] H. L. Skriver and N. Rosengaard, Phys. Rev. B **46**, 7157 (1992).
[20] G. Kresse and D. Joubert, Phys. Rev. B **59**, 1758 (1999).
[21] P. E. Blöchl, Phys. Rev. B **50**, 17953 (1994).
[22] J. P. Perdew, K. Burke, and M. Ernzerhof, Phys. Rev. Lett. **77**, 3865 (1996).

[23] H. J. Monkhorst and J. D. Pack, Phys. Rev. B **13**, 5188 (1976).
[24] I. Popov, G. Seifert, and D. Tománek, Phys. Rev. Lett. **108**, 156802 (2012).
[25] W. Liu, J. Wei, X. Sun, and H. Yu, Crystals **3**, 257 (2013).
[26] Y. Pan, Y. Wang, L. Wang, H. Zhong, R. Quhe, Z. Ni, M. Ye, W.-N. Mei, J. Shi, and W. Guo, Nanoscale **7**, 2116 (2015).
[27] Y. Pan, Y. Wang, M. Ye, R. Quhe, H. Zhong, Z. Song, X. Peng, D. Yu, J. Yang, and J. Shi, Chem. Mater. **28**, 2100 (2016).
[28] X. Ji, J. Zhang, Y. Wang, H. Qian, and Z. Yu, Phys. Chem. Chem. Phys. **15**, 17883 (2013).
[29] J. Kang, W. Liu, D. Sarkar, D. Jena, and K. Banerjee, Phys. Rev. X **4**, 031005 (2014).
[30] Y. Liu, H. Xiao, and W. A. Goddard III, J. Am. Chem. Soc. **138**, 15853 (2016).
[31] P. Khomyakov, G. Giovannetti, P. Rusu, G. V. Brocks, J. Van den Brink, and P. J. Kelly, Phys. Rev. B **79**, 195425 (2009).